Radiocarbon, Vol 62, Nr 1, 2020, p 189–196 DOI:10.1017/RDC.2019.78

RADIOCARBON MAP OF A BOMB-PEAK LABELED HUMAN EYE

Laszlo Rinyu[1]* • Robert Janovics[1] • Mihaly Molnar[1] • Zoltan Kisvarday[2] • Adam Kemeny-Beke[3]

[1]Isotope Climatology and Environmental Research Centre (ICER), Institute for Nuclear Research (ATOMKI), Hungarian Academy of Sciences, Bem ter 18/c, 4026 Debrecen, Hungary
[2]MTA-Debreceni Egyetem Neuroscience Research Group, Nagyerdei krt. 98, 4032 Debrecen, Hungary
[3]Department of Ophthalmology, Faculty of Medicine, University of Debrecen, Nagyerdei krt. 98, 4032 Debrecen, Hungary

ABSTRACT. The $^{14}C/^{12}C$ ratio of living organisms is largely determined by the $^{14}C/^{12}C$ ratio of consumed diet as well as by the atmospheric ^{14}C concentration together with the body's metabolic processes. The measured ^{14}C content of living matter compared to the atmospheric radiocarbon level can provide invaluable information about developmental processes. Our aim was to determine the ^{14}C content of ten different tissues of the human eye using the ^{14}C bomb-pulse dating signature. The ^{14}C content of the atmosphere, so called ^{14}C "bomb-pulse" has labeled humanity offering an opportunity to determine these special formation, turnover and substitution courses in biology. The results allowed us to construct a ^{14}C map of the bomb-peak labeled human eye. According to the anatomical location of the tissues, an unexpected picture emerged as in moving from the outer parts towards the inner parts of the eye, the ^{14}C content of each tissue decreased. The data presented here are compatible with the view that the oldest parts of the eye are the sclera, the limbus and the cornea, in this order, and moving further inside, the youngest tissue of the eye is the retina.

KEYWORDS: bomb-peak dating, human eye, isotope analysis, radiocarbon dating, tissue development.

INTRODUCTION

Traditionally, artificial ^{14}C labeling techniques are used in biomedical research to understand biological processes at the molecular level, though the high price and scarceness of these labeled substrates significantly limit the implementation of these studies. However, due to the atmospheric testing of the nuclear weapons the amount of the radiocarbon content in the atmosphere nearly doubled within a few years (Levin and Kromer 2004; Levin et al. 2008; Hua et al. 2013) and this was incorporated into organisms that lived after the 1960s. After the maximum in the 1960s and 1970s, the excess of ^{14}C decreased rapidly in the atmosphere offering a great opportunity for assessing the carbon turnover rates or the molecular turnover rates of different kinds of biological tissues (Libby et al. 1964; Nydal et al. 1971; Harkness and Walton 1972; Stenhouse and Baxter 1977; Druffel and Mok 1983; Wild et al. 2000; Geyh et al. 2001; Georgiadou and Stenström 2010; Stenström et al. 2010; Falso and Buchholz 2013). The execution of these specific tests, which utilize the bomb-^{14}C labeling technique, is slowly running out of time because of the availability of the ^{14}C tracer which is constrained by the date of the atmospheric nuclear tests. In line with this the number of the available donors whose birth dates are in the appropriate age range (between 1960 and 1990) is decreasing, as well.

The ^{14}C content of living organisms remains proportional with the atmospheric level due to the continuous metabolic turnover, substitution and realignment of tissue components. Previous studies have established that some human tissues do not undergo any changes after their initial formation e.g. dental enamel (Spalding et al. 2005; Cook et al. 2006) while there are tissue types which keep the changes after reaching maturation at a reduced level and within a well-defined time interval, e.g. the human crystalline lens (Lynnerup et al. 2008; Kjeldsen et al. 2010).

Here, we investigated ten tissue components of the human eye to unveil and determine their virtual ^{14}C ages using the ^{14}C bomb-pulse dating as reference. The ^{14}C map obtained here for

*Corresponding author. Email: rinyu.laszlo@atomki.mta.hu.

the human eye as well as the carbon exchange rates of the investigated tissues allowed to expose so far unknown developmental relationships.

MATERIALS AND METHODS

This study was approved by the Scientific Council of Health, Scientific and Research Ethics Committee of the University of Debrecen (reference number: 63571-1/2017/EKU).

Donor Selection

A key requirement of this study was to find an appropriate subject for the investigations. Specifically, very strict inclusion criteria were applied, i.e. the donor's birth date had to be close enough to the time range when the nuclear weapon tests reached their peak, all relevant anamnestic and nutritional history had to be available, and any factor that could significantly modify intrabulbar metabolism had to be excluded. Only one donor was found during the selection period who met the above criteria. He was born April 25, 1965, had lived in an agricultural area of Hungary and had a typical provincial diet. He died in March 23, 2013. This subject had no known long-term chronic diseases during his life and systematic drug consumption could also be excluded, which would have influenced the ^{14}C content of the investigated tissues. All in all, the donor may be regarded as a representative of the average population of the Great Hungarian Plain area.

Sample Collection and Purification

The removal of the eyes of the human donor and the separation of the tissue samples were performed on the date of the subject's death in compliance with the ethics scheme of the University of Debrecen. The enucleation of the eyeballs was carried out carefully with special regard to avoid any contamination with surrounding tissues within less than 6 hr from the time point of death. The process of enucleation took approximately 15 min, and immediately the preparation of tissues was performed by sterile instruments for each tissue. Then the separated tissue samples were frozen at –80ºC in order to prevent potential post-mortem degradation of the tissues.

The water content of the tissues was removed by freeze-drying (at 1–5 mbar pressure, for 24 hr) using a UNICRYO MC2L-60. The dry matter ratios of the samples depend on the particular histological type (Table 1). In order to test and verify reproducibility of the chemical extraction and the measurement processes, i.e. two independent measurements, each tissue sample of the eyeball was divided in two parts and stored separately.

A former study of Kjeldsen et al. (2010) showed that the formation processes of the outer capsule and the nucleus of the human eye lens take place on highly different timescales. Consequently, their ^{14}C content must also differ. In order to confirm this feature, we separated the outer capsule of the eye lens from the nucleus after the freeze-drying process. The tissue separation was helped by their different colors gained during the freeze-drying process. There was no chemical pretreatment, after the freeze-drying process. The dry content of the tissue samples and standards (IAEA-C7 and –C9 Le Clercq et al. 1998; Hogg et al. 1995; Scott 2003, handled/prepared in the same way as tissue samples) were combusted in evacuated quartz tubes with CuO at 1000ºC for 10 min. The extraction of the generated CO_2 from the other combustion gases was carried out on a cryogenic gas preparation line (for details, see Molnar et al. 2013a). The separated CO_2 gas was

https://doi.org/10.1017/RDC.2019.78 Published online by Cambridge University Press

Table 1 Dry matter content of the tissues of the human eye investigated.

Type	Dry matter percentage (%)	Dry matter amount (mg)
Choroid	11	23.3
Conjunctiva	18	43.4
Cornea	14	11.6
Crystalline lens	32	64.0
Iris	25	4.2
Limbus	21	20.7
Optic nerve	28	8.0
Muscle	23	6.6
Retina	3	33.1
Sclera	28	315.5

converted to graphite in a sealed tube according to the graphitization method introduced by Rinyu et al. (2013). In the case of less than 100 micrograms carbon in the tissue sample, the zinc micro-graphitization technique was used (Rinyu et al. 2015).

Measurement of the Radiocarbon Content

The measurements of the ^{14}C contents were carried out on a MICADAS (MIni CArbon DAting System, Synal et al. 2004, 2007) type accelerator mass spectrometer (Molnar et al. 2013b). Graphite targets which were prepared from NIST-SRM-499°c oxalic acid standard (134.07 pMC, $\delta^{13}C = -17.78 \pm 0.08$ ‰) were used as normalization standard and from fossil ^{14}C-free CO_2 gas (Linde AG, Répcelak, Hungary, 4.5 purity, $\delta^{13}C = -3.78 \pm 0.08$‰) were used as instrument blank. For determining the amount of modern versus dead carbon, i.e. recently incorporated carbon, representing contamination during the chemical pre-treatment process, chemical standards with well-known ^{14}C activity were employed (IAEA C7 and C9, Le Clercq et al. 1998; Hogg et al. 1995; Scott 2003) and measured together with the samples in the same magazines.

The Fraction Modern ($F^{14}C$) (Mook and van der Plicht 1999; Stenström et al. 2011; Reimer et al. 2013) unit was used to compare the ^{14}C contents of the individual tissues.

Calculating Virtual Age

The $F^{14}C$ unit does not depend on the year of the measurement and is commonly used for ^{14}C measurements and date calibration of post-bomb samples. All ^{14}C results were processed using the BATS AMS data evaluation software developed by Lukas Wacker, ETH Zurich (Wacker et al. 2010).

Calibration of the resulting $F^{14}C$ value is required in order to determine the calendar age of the investigated sample. CALIBomb program was used to calibrate post-bomb samples. Calibrated calendar year intervals were obtained using IntCal13 data set (Reimer et al. 2013) with Levin (Levin and Kromer 2004; Levin et al. 2008) bomb curve extension (IntCal13/Levin) and IntCal13 data set with NHZ1 (Hua et al. 2013) bomb curve extension (IntCal13/NH Zone 1). Contemporary level of ^{14}C in Hungary is continuously monitored by our research group (Major et al. 2018) using atmospheric ^{14}C analyses. Measured values

https://doi.org/10.1017/RDC.2019.78 Published online by Cambridge University Press

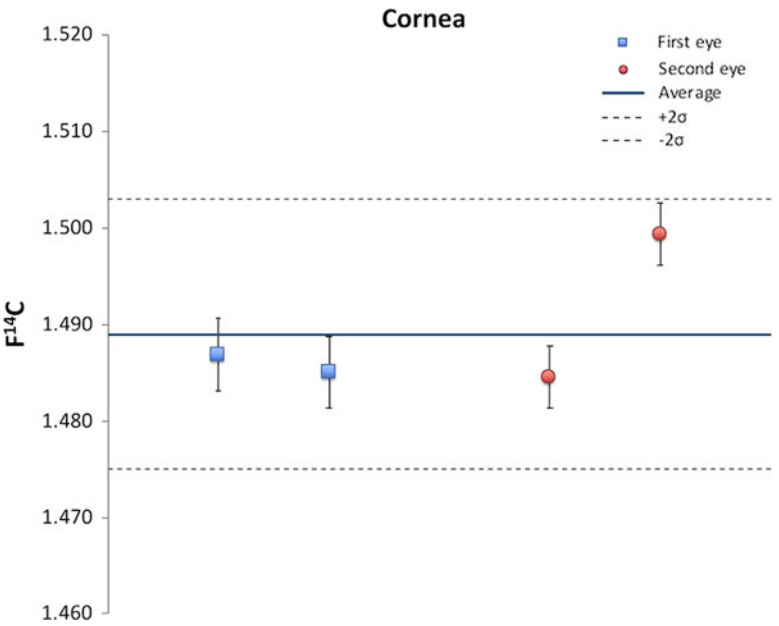

Figure 1 Test of the reproducibility of the chemical extraction and the measurement processes; ^{14}C results of four independent cornea samples.

in Debrecen city and also a rural station in western Hungary (Hegyhátsál) shows very good agreement with the Jungfraujoch continental background station.

The resulting calendar year intervals were named "virtual age" of the given tissue. This year interval is not the real age of the tissue. This year interval, which was determined by the $F^{14}C$ value of the tissue sample, characterizes those living organisms which died during the given annual period and till that time they maintained an active relationship—by metabolism—with the atmospheric ^{14}C concentration. Moreover, the virtual age characterizes the whole tissue as a unit, which has many unique building parts with different ^{14}C content and this value is also determined by the tissue related metabolic exchange processes.

RESULTS AND DISCUSSION

Four individual cornea samples of the cadaver were processed in order to investigate the reliability of the chemical extraction procedure and the measurement process (Figure 1). The average of the four $F^{14}C$ values was 1.489 and the standard deviation was 0.007. At the 0.025 significance level the four measured values cannot be distinguished.

In order to examine measurement consistencies, we used a previously-developed protein formation function for the crystalline lens (Kjeldsen et al. 2010). Considering that the donor died in January 2013, and that a one-year shift is commonly observed in case of the dietary ^{14}C content relative to the atmospheric ratio, it can be calculated that the ^{14}C content of the nucleus of the crystalline lens should be 1.601 $F^{14}C$ (Kjeldsen et al. 2010). Based on two independent measurements of the nucleus of the crystalline lens taken from our subject the average ^{14}C content was 1.610 ± 0.010 $F^{14}C$, which is close to the above-mentioned theoretical value.

https://doi.org/10.1017/RDC.2019.78 Published online by Cambridge University Press

Table 2 shows all the measured values obtained for the different tissue types of the same eyeball. Of these, there are structures such as the nucleus of the crystalline lens, sclera, limbus and cornea which have relatively high ^{14}C contents. Their calibrated virtual age intervals are quite close to the date of birth. For example, the cornea has the fourth closest time interval to the date of birth, i.e. approximately 9 yr (8.37 yr). This means that tissues possessing relatively high amounts of ^{14}C slowed down their metabolism, formation and substitution processes greatly. It follows that the formation function of these tissues can be determined with high accuracy just as it has been made for the crystalline lens' (Lynnerup et al. 2008; Kjeldsen et al. 2010).

The ^{14}C content and the virtual age intervals of the sclera are in line with the measured values of the nucleus of the crystalline lens. However, its more complex structure requires compound specific investigation in order to develop the appropriate model of the formation function of the sclera. Moreover, it should be noted that the mathematical models describing the above attributes cannot be developed and implemented without extensive and well-organized sample collection and measurements using donors with various lifespan and birth dates.

Interestingly, the iris has an intermediate calibrated virtual age, suggesting that the development and exchange processes in this tissue did not stop completely, and the metabolic process worked with higher intensity in this tissue. Clearly, the retina is the virtually youngest tissue of the eye, as expected. Also, interesting but not entirely surprising, is the fact that the virtual age of the outer capsule of the crystalline lens is very close to the virtual age of the retina. Nonetheless, both values are located more than 10 yr away from the date of death, probably due to the decreased substitution and metabolic exchange rate in these tissues.

The measured ^{14}C data of the nucleus and the outer capsule of the crystalline lens show nicely that the epithelial basement membrane isolates the inner part of the crystalline lens completely from the surrounding tissues and there is no sign of transport of metabolites in this area (Table 2).

Finally, considering the anatomical location and spatial relationship of the tissues of different virtual ages an interesting picture emerges (Figure 2). As we move from the outer parts towards the inner parts of the eyeball, with the exception of the nucleus of the crystalline lens, the virtual age of tissues is getting lower and lower. The oldest parts of the eye are the sclera, the limbus and the cornea, in this order, whereas further inside we reach the retina, which is the youngest tissue of the human eye. These findings significantly modify current concepts of eye development in terms of the evolution times of different tissue types. The main developmental process conjectured here using the ^{14}C technique is compatible with a delayed maturation of the tissues as we move from the outer parts towards the inner parts of the eyeball with the exception of the outer capsule of the lens. These data add further information to the understanding of postnatal development of the eye.

CONCLUSIONS

The measured ^{14}C content of the samples confirmed that the completion time and the rate of formation, substitution and realignment of the tissues vary widely. In the eye there are tissue types in which developmental changes rapidly slow down and reach steady state. For each tissue type, the above changes take place during a characteristic time interval. The virtual ^{14}C ages which were determined from the measured ^{14}C content have an ultimate importance in confirming tissue specific evolution of the human eye. The younger virtual

https://doi.org/10.1017/RDC.2019.78 Published online by Cambridge University Press

Table 2 The measured $F^{14}C$ values of the different tissues and their calibrated virtual age intervals. The 1σ and 2σ intervals are given in correspondence to the 68.2% and 95.4% probability of the output from CALIBomb, respectively. Calibrated calendar year intervals were obtained using IntCal13 data set (Reimer et al. 2013) with Levin (Levin and Kromer 2004, Levin et al. 2008) bomb curve extension (IntCal13/Levin) and IntCal13 data set with NHZ1 (Hua et al. 2013) bomb curve extension (IntCal13/NH Zone 1).

	AMS ^{14}C results		IntCal13/Levin		IntCal13/NH Zone 1	
Tissue	$F^{14}C$	±	1σ	2σ	1σ	2σ
Nucleus of crystalline lens*	1.610	0.010	1967.7–1968.0	1966.8–1968.5	1967.6–1968.7	1966.8–1970.7
Sclera	1.582	0.003	1967.9–1968.6	1967.9–1968.6	1967.9–1969.8	1967.7–1971.5
Limbus	1.537	0.004	1969.1–1970.8	1968.8–1971.6	1968.8–1971.6	1968.7–1971.8
Cornea*	1.489	0.004	1971.1–1972.5	1971.0–1972.5	1971.1–1972.9	1971.0–1973.7
Iris	1.314	0.003	1977.9–1979.6	1977.8–1979.8	1977.9–1979.1	1976.2–1979.7
Conjunctiva	1.261	0.003	1980.2–1982.7	1980.1–1982.7	1980.2–1982.0	1979.9–1982.4
Optic nerve	1.200	0.003	1984.1–1987.6	1984.0–1987.7	1985.0–1986.8	1984.1–1987.7
Muscle	1.167	0.003	1986.1–1990.6	1986.1–1990.7	1988.8–1990.1	1987.1–1990.9
Choroid	1.132	0.003	1991.1–1995.7	1990.7–1995.7	1992.1–1994.7	1991.2–1995.8
Outer capsule of lens*	1.102	0.008	1995.3–2000.2	1995.3–2001.0	1997.3–1999.9	1996.1–2000.7
Retina*	1.100	0.003	1995.3–2000.9	1995.3–2001.5	1997.9–2000.1	1996.1–2000.8

*These results are the average of two or more measurements of individually handled sample.

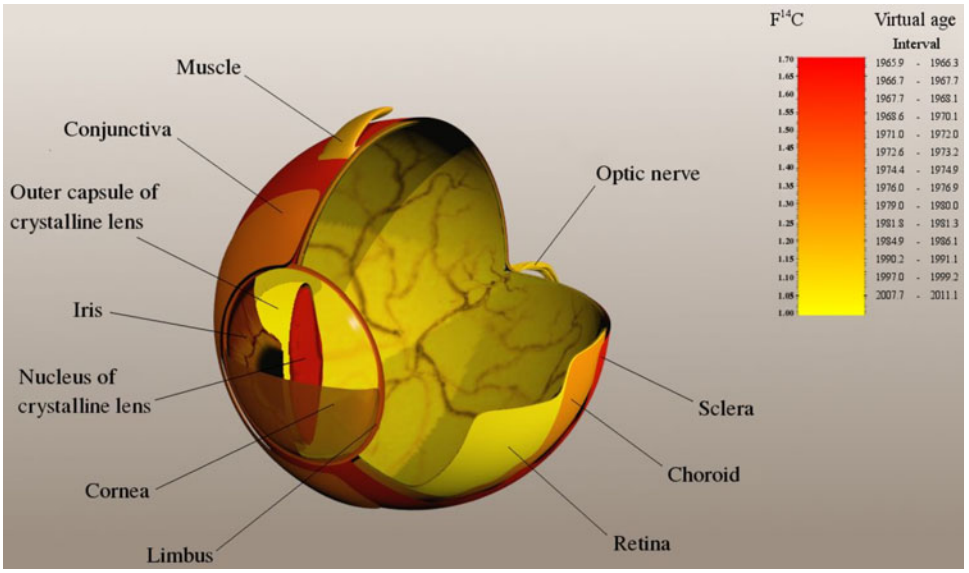

Figure 2 ^{14}C map of a bomb-peak labeled human eye. The gamut represents the ^{14}C content (in $F^{14}C$ unit) and virtual age interval. The darker color means higher ^{14}C concentration and higher virtual age. Virtual age is defined as the calibrated calendar date in which the atmospheric ^{14}C concentration was the same as measured in the given tissue.

age as well as lower $F^{14}C$ value means that the given tissue maintains higher relationship with the nutrient transport and/or it has tighter connection with the blood vessel system. It may indicate that tissues that are virtually younger have a higher flow of contemporary nutrients into the cells. For example, the younger value of the retina could be explained by a higher fraction of contemporary nutrients than e.g. in the lens, which should have no flow of nutrients into it. Based on our ^{14}C measurements, i.e. the amount of ^{14}C, the oldest parts of the human eye are the nucleus of the crystalline lens, the sclera, the limbus and the cornea. Conversely, the youngest tissue of the human eye is the retina as has been suggested by traditional developmental studies. As a next step of this study DNA analysis of specific cell types could help to estimate the average age of the cells.

ACKNOWLEDGMENTS

This work was supported by the European Union and the State of Hungary, co-financed by the European Regional Development Fund (GINOP-2.3.2.-15-2016-00009 "ICER") and the Hungarian Brain Research Program (NAP2, 2017-1.2.1-NKP-2017-00002). The authors would like to thank Judit Orsovszki for the creation of Figure 2. None of the authors has any potential financial conflict of interest related to this manuscript.

REFERENCES

Cook GT, Dunbar E, Black SM, Xu S. 2006. A preliminary assessment of age at death determination using the nuclear weapons testing ^{14}C activity of dentine and enamel. Radiocarbon 48(3):305–313.

Druffel EM, Mok HYI. 1983. Time history of human gallstones: application of the post–bomb radiocarbon signal. Radiocarbon 25(2):629–636.

Falso MJS, Buchholz BA. 2013. Bomb pulse biology. Nuclear Instruments and Methods in Physics Research B 294:666–670.

Georgiadou E, Stenström K. 2010. Bomb-pulse dating of human material: modeling the influence of diet. Radiocarbon 52(2–3):800–807.

Geyh MA. 2001. Bomb radiocarbon dating of animal tissues and hair. Radiocarbon 43(2b):723–730.

https://doi.org/10.1017/RDC.2019.78 Published online by Cambridge University Press

Harkness DD, Walton A. 1972. Further investigation of the transfer of bomb ^{14}C to man. Nature 240:302–303.

Hogg AG, Higham T, Robertson S, Beukens R, Kankainen T, McCormac FG, van der Plicht J, Stuiver M. 1995. Radiocarbon age assessment of a new, near background IAEA ^{14}C quality assurance material. Radiocarbon 37(2):797–803.

Hua Q, Barbetti M, Rakowski AZ. 2013. Atmospheric radiocarbon for the period 1950–2010. Radiocarbon 55(4):2059–2072.

Kjeldsen H, Heinemeier J, Heegaard S, Jacobsen C, Lynnerup N. 2010. Dating the time of birth: a radiocarbon calibration curve for human eye-lens crystallines. Nuclear Instruments and Methods Physics Research B 268:1303–1306.

Le Clercq M, van der Plicht J, Gröning M. 1998. New ^{14}C reference materials with activities of 15 and 50 pMC. Radiocarbon 40(1):295–297.

Levin I, Kromer B. 2004. The tropospheric $^{14}CO_2$ level in mid-latitudes of the Northern Hemisphere (1959–2003). Radiocarbon 46(3):1261–1272.

Levin I, Hammer S, Kromer B, Meinhardt F. 2008. Radiocarbon observations in atmospheric CO_2: determining fossil fuel CO_2 over Europe using Jungfraujoch observations as background. Science of the Total Environment 391(2–3):211–216.

Libby WF, Berger R, Mead JF, Alexander GV, Ross JF. 1964. Replacement rates for human tissue from atmospheric radiocarbon. Science 146(3648):1170–1172.

Lynnerup N, Kjeldsen H, Heegraad S, Jacobsen C. and Heinemeier J. 2008. Radiocarbon dating of the human eye lens crystallines reveal proteins without carbon turnover throughout life. PLoS ONE 3(1):e1529.

Major I, Haszpra L, Rinyu L, Futó I, Bihari Á, Hammer S, Jull AJT, Molnar M. 2018. Temporal variation of atmospheric fossil and modern CO_2 excess at a Center European Rural Tower Station between 2008 and 2014. Radiocarbon 60(5):1285–1299.

Molnar M, Janovics R, Major I, Orsovszki J, Gönczi R, Veres M, Leonard AG, Castle SM, Lange TE, Wacker L, Hajdas I, Jull AJT. 2013a. Status report of the new AMS ^{14}C sample preparation lab of the Hertelendi Laboratory of Environmental Studies (Debrecen, Hungary). Radiocarbon 55(2–3):665–676.

Molnar M, Rinyu L, Veres M, Seiler M, Wacker L, Synal HA. 2013b. EnvironMICADAS: a mini ^{14}C AMS with enhanced gas ion source interface in the Hertelendi Laboratory on Environmental Studies(HEKAL), Hungary. Radiocarbon 55(2–3):338–344.

Mook WG, van der Plicht J. 1999. Reporting ^{14}C activities and concentrations. Radiocarbon 41(3):227–239.

Nydal R, Lövseth K, Syrstad O. 1971. Bomb ^{14}C in the human population. Nature 232:418–421.

Reimer PJ, Bard E, Bayliss A, Beck JW, Blackwell PG, Bronk Ramsey C, Buck C, Cheng H, Edwards RL, Friedrich M, Grootes PM, Guilderson TP, Haflidason H, Hajdas I, Hatté C, Heaton TJ, Hoffmann DL, Hogg AG, Hughen KA, Kaiser KF, Kromer B, Manning SW, Niu M, Reimer RW, Richards DA, Scott EM, Southon JR, Staff RA, Turney CSM, van der Plicht J. 2013. IntCal13 and Marine13 radiocarbon age calibration curves 0–50,000 years cal BP. Radiocarbon 55(4):1869–1887.

Rinyu L, Molnar M, Major I, Nagy T, Veres M, Kimak A, Wacker L, Synal HA. 2013. Optimization of sealed tube graphitization method for environmental ^{14}C studies using MICADAS. Nuclear Instruments and Methods in Physics Research B 294:270–275.

Rinyu L, Orsovszki G, Futo I, Veres M, Molnar M. 2015. Application of zinc sealed tube graphitization on sub–milligram samples using EnvironMICADAS. Nuclear Instruments and Methods in Physics Research Section B 361:406–413.

Scott EM. 2003. The Fourth International Radiocarbon Intercomparison (FIRI). Radiocarbon 45(2): 135–150.

Spalding KL, Buchholz BA, Bergman LE, Druid H, Frisen J. 2005. Forensics: age written in teeth by nuclear tests. Nature 437(7057):333–337.

Stenhouse MJ, Baxter MS. 1977. Bomb ^{14}C a biological tracer. Nature 267:828–832.

Stenström K, Skog G, Nilsson CM, Hellborg R, Svegborn SL, Georgiadou E, Mattsson S. 2010. Local variations in ^{14}C—How is bomb-pulse dating of human tissues and cells affected? Nuclear Instruments and Methods in Physics Research B 268:1299–1302.

Stenström K, Skog G, Georgiadou E, Genberg J, Johansson A. 2011. A guide to radiocarbon units and calculations. Internal report, Lund University LUNFD6 (NFFR–3111):1–17.

Synal HA, Döbeli M, Jacob S, Stocker M, Suter M. 2004. Radiocarbon AMS towards its lower-energy limits. Nuclear Instruments and Methods in Physics Research B 223–224:339–345.

Synal HA, Stocker M, Suter M. 2007. MICADAS: a new compact radiocarbon AMS system. Nuclear Instruments and Methods in Physics Research B 259:7–13.

Wacker L, Christl M, Synal HA. 2010. Bats: a new tool for AMS data reduction. Nuclear Instruments and Methods in Physics Research B 268:976–979.

Wild EM, Arlamovsky KA, Golser R, Kutschera W, Priller A, Puchegger S, Rom W, Steier P, Vycudilik W. 2000. ^{14}C dating with the bomb peak: an application to forensic medicine. Nuclear Instruments and Methods in Physics Research B 172:944–950.

https://doi.org/10.1017/RDC.2019.78 Published online by Cambridge University Press